International Journal of Applied Earth Observation and Geoinformation 147 (2026) 105170

Contents lists available at ScienceDirect

International Journal of Applied Earth Observation and Geoinformation

journal homepage: www.elsevier.com/locate/jag

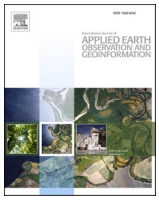

Salinity-induced global pattern of atmospheric water constraints on mangrove photosynthetic activity revealed by time series Sentinel-2 data

Yanjie Liu [a,b,c,d], Yueting Deng [a,b,c,e], Hui Luo [b,e], Nengwang Chen [a,b,c,d,e,f], Yougan Chen [f,g], Zhenong Jin [h,i], Xu Wang [j], Hongsheng Zhang [k], Xudong Zhu [a,b,c,d,e,f,*]

[a] State Key Laboratory of Marine Environmental Science, Xiamen University, Xiamen, Fujian, China
[b] National Observation and Research Station for the Taiwan Strait Marine Ecosystem (Xiamen University), Zhangzhou, Fujian, China
[c] Key Laboratory of the Coastal and Wetland Ecosystems (Ministry of Education), Xiamen University, Xiamen, Fujian, China
[d] Coastal and Ocean Management Institute, Xiamen University, Xiamen, Fujian, China
[e] College of the Environment and Ecology, Xiamen University, Xiamen, Fujian, China
[f] Shenzhen Research Institute of Xiamen University, Shenzhen, Guangdong, China
[g] College of Ocean and Earth Sciences, Xiamen University, Xiamen, Fujian, China
[h] Institute of Ecology, College of Urban and Environmental Science, Peking University, Beijing, China
[i] State Key Laboratory of Vegetation Structure, Function and Construction (VegLab), Peking University, Beijing, China
[j] School of Civil and Environmental Engineering, Harbin Institute of Technology, Shenzhen, Shenzhen, Guangdong, China
[k] Department of Geography, The University of Hong Kong, Hong Kong, China

ARTICLE INFO

Keywords:
Mangrove
Red-edge position
Atmospheric drought stress
Seawater salinity
Geoinformation analysis

ABSTRACT

Atmospheric drought stress limits mangrove photosynthetic activity, and this constraint can be further amplified by high salinity, yet their combined global effects remain poorly understood. Here, we integrated multi-source Earth observation and geoinformation datasets, including Sentinel-2 red-edge position (a proxy for canopy photosynthetic activity), vapor pressure deficit from TerraClimate, seawater salinity from Copernicus reanalysis, to investigate how salinity regulates the sensitivity of mangrove photosynthesis to atmospheric drought stress during 2019–2023. Datasets were harmonized and analyzed through reproducible geoinformation workflows at 10 m–0.5° resolutions, enabling large-scale coupling analyses between remote sensing proxies and climate drivers. We found that drought stress constrained mangrove photosynthetic activity worldwide, with stronger limitations in tropical savannahs than in tropical rainforests. Marine mangroves exposed to persistent high salinity were more sensitive than estuarine mangroves influenced by freshwater inflow. These results reveal a global pattern in which salinity amplifies atmospheric water constraints on mangrove photosynthesis. Mangroves in dry climates and high-salinity habitats are therefore most vulnerable to future warming and drying. Our findings confirm that integrating multi-source satellite observations with geoinformation analysis provides an effective, large-scale approach for assessing vegetation vulnerability and identifying conservation priorities in climate-sensitive mangrove ecosystems.

1. Introduction

Global warming caused by human activities has resulted in significant changes in temperature, rainfall, wind direction, and sea level over the past century (Stocker, 2014). As one of the coastal blue carbon ecosystems, mangroves are among the natural ecosystems with the strongest carbon sequestration capacity (Friess et al., 2019; Rovai et al., 2018; Su, Friess, & Gasparatos, 2021). Although mangroves only account for 0.5% of the global coastal area, their contribution to blue carbon sequestration makes them one of the preferred natural-based solutions for mitigating climate change (Duarte et al., 2013; Lovelock et al., 2024; Rosentreter et al., 2023). However, mangroves also face severe challenges brought by climate change, and the harsh habitats at their land-sea interface make them more vulnerable to the impacts of climate change (Sharma et al., 2020; Zhang et al., 2024). The photosynthetic activity of mangroves is sensitive to various environmental

* Corresponding author at: College of the Environment and Ecology, Xiamen University, Xiamen, Fujian 361102, China.
E-mail address: xdzhu@xmu.edu.cn (X. Zhu).

https://doi.org/10.1016/j.jag.2026.105170
Received 2 October 2025; Received in revised form 19 December 2025; Accepted 12 February 2026

stresses, such as high temperature (Chung et al., 2023), sea-level rise (Lovelock et al., 2015), atmospheric drought (Gou et al., 2024), and high salinity (Cui et al., 2018). In the future, climate change will make drought stress more frequent and severe. Therefore, studying atmospheric water constraints on mangrove photosynthetic activity can help understand the response and adaptation of mangroves to climate change.

Vapor pressure deficit (VPD), a common metric reflecting atmospheric water demand or the degree of atmospheric drought stress, is expected to increase continuously with global warming (Shekhar et al., 2023). Elevated VPD affects mangrove photosynthesis through several physiological mechanisms (Reef & Lovelock, 2015). When there is sufficient water in the atmosphere, mangroves allocate more resources to leaf development and hydraulic structure, which is more conducive to photosynthesis and canopy growth (Granados-Martínez et al., 2021; Li et al., 2025). Extreme VPD is found to have a significant impact on the stomatal opening of plants (López, Way, & Sadok, 2021). Under high VPD conditions, plants tend to reduce stomatal opening to minimize water loss (Grossiord et al., 2020), while the decrease in stomatal opening can also hinder the uptake of carbon dioxide (CO_2), thereby limiting photosynthesis and plant growth (Sulman et al., 2016; Wang et al., 2025). Meanwhile, when stomata close, transpiration decreases, leading to increased leaf temperatures (Gahir, Bharath, & Raghavendra, 2021). This temperature rise can enhance photorespiration, thereby reducing photosynthetic efficiency. Previous studies have reported the inhibition effect on mangrove photosynthesis induced by high VPD (Gnanamoorthy et al., 2020; Gou et al., 2024; Granados-Martínez et al., 2021). It has also been reported that increasing VPD will lead to a decrease in canopy light use efficiency in mangrove forests (Liu & Zhu, 2024; Rodda et al., 2022; Zhu & Zhu, 2025). Meanwhile, some studies suggest that the correlation between mangrove carbon uptake and VPD may be regulated by other environmental factors (Xu et al., 2025). Gou et al. (2024) found that high temperature and radiation can exacerbate the atmospheric drought stress caused by the increase in VPD. However, these studies focus on observation data from single or multiple sites, making it difficult to compare the atmospheric water constraints on mangrove photosynthetic activity across different habitats at a regional or global scale.

High salinity, despite mangroves being halophytic, remains one of the major abiotic stresses influencing their physiology (Perri et al., 2019; Rovai et al., 2021). The physiological response of mangroves to high salinity is like that of terrestrial vegetation experiencing extremely low soil moisture, as the low osmotic potential in high-salinity soil limits the water supply for mangroves (Alongi, 2009). In comparison with mangroves grown in low salt environments, mangroves in high salt environments often have lower stomatal conductance, transpiration, and internal CO_2 concentration, resulting in lower overall photosynthetic rates (Krauss & Ball, 2013; Nguyen et al., 2015). However, there are significant regional differences in the sensitivity of mangrove photosynthesis to high salinity and atmospheric drought stress, mainly related to climate zones and hydrological environments (Alvarado-Barrientos et al., 2021; Liu and Lai, 2019). Ward et al. (2016) highlighted that the impact of climate change factors on mangrove ecosystems varied significantly in different regions and pointed out that mangroves exhibited different ecological characteristics and responses to environmental stresses under different geographical locations and climatic conditions. The differences in estuarine and coastal environments, especially hydrological differences, result in varying carbon fluxes of mangroves growing in these two types of environments, with salinity being considered the main cause (Cotovicz et al., 2024; Donato et al., 2011; Liu et al., 2025). Mangroves grown in marine environments, such as arid coastlines and hypersaline lagoons, are exposed to higher and more constant salinity levels due to limited freshwater inflow (Fig. 1a). Higher salinity intensifies root-level water stress, reduces stomatal conductance, and amplifies the effects of atmospheric water constraints on mangrove carbon assimilation (Reef & Lovelock, 2015). In contrast, mangroves grown in estuarine environments typically benefit from lower and more variable salinity due to the mixing of freshwater from rivers with tidal seawater (Fig. 1b). Lower salinity reduces osmotic stress on mangrove roots, enhancing their capacity to take up water, maintain open stomata (Krauss et al., 2008), and support higher photosynthetic rates under atmospheric water constraints.

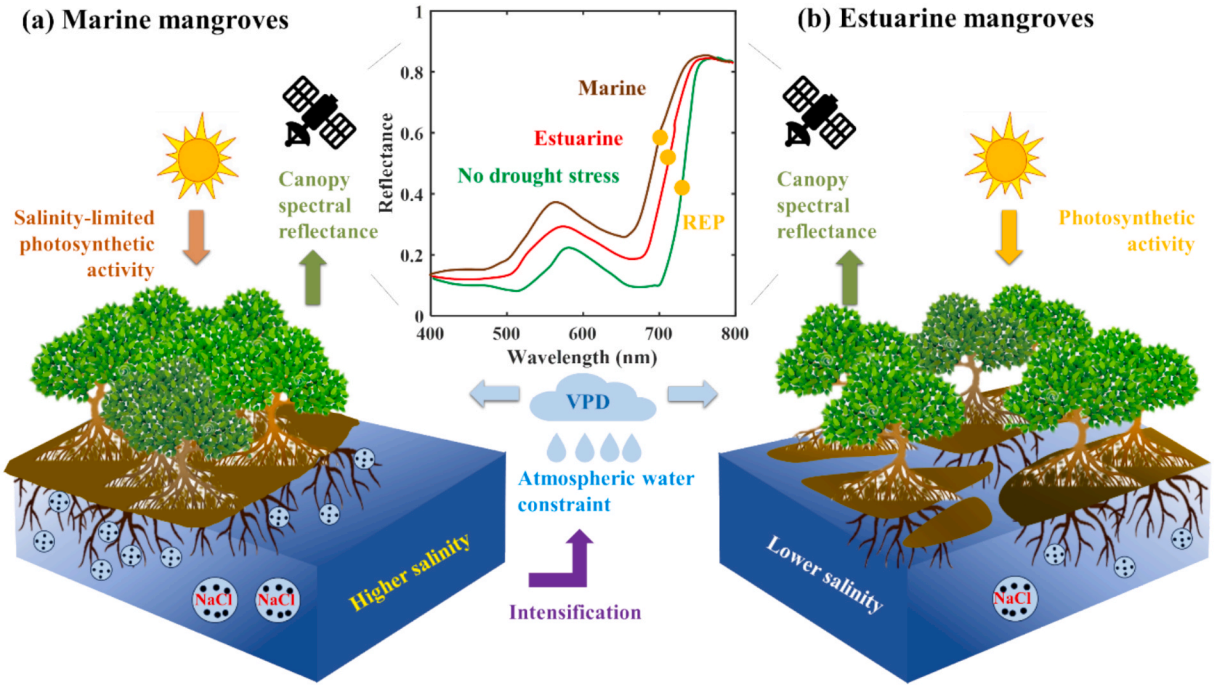

Fig. 1. Differential atmospheric water constraints on mangrove photosynthetic activity between marine (a) and estuarine (b) habitats. A stronger blue shift in the red-edge position (REP) of canopy reflectance spectra with increasing vapor pressure deficit (VPD) occurs in marine mangroves experiencing higher salinity. (For interpretation of the references to colour in this figure legend, the reader is referred to the web version of this article.)

In terms of using remote sensing spectral indices to characterize vegetation photosynthetic activity, the red-edge band has been considered an excellent proxy for monitoring seasonal changes in vegetation chlorophyll content and photosynthetic capacity due to its sensitivity to leaf and canopy chlorophyll content (Croft et al., 2017; Luo et al., 2019). The efficiency of photosynthesis is closely related to the amount of chlorophyll, and this affects the red-edge region of the reflectance spectrum. Higher chlorophyll content typically results in a red-edge shift towards longer wavelengths, indicating an enhanced photosynthetic capacity (Ustin & Jacquemoud, 2020; Yang et al., 2024). For instance, Zhou et al. (2021) found that the position of the red-edge in citrus can indicate the changes in photosynthetic capacity caused by water stress. Yi et al. (2017) assessed the ability of spectral reflectance in indicating leaf photosynthetic efficiency and showed the advantages of red-edge bands. Liu & Zhu (2024) also found that the red-edge band of mangrove forests underwent a "red-edge blue shift" phenomenon in high VPD environments, indicating that the movement of the red-edge position (REP) can reflect the changes in mangrove photosynthetic activity.

To fill the knowledge gap on the global pattern of atmospheric water constraints on mangrove photosynthetic activity, this study used Sentinel-2 remote sensing data and other spatiotemporal data from the past 5 years (2019–2023) to firstly analyze the monthly coupling (represented by Pearson correlation analysis) between global 10-m mangrove pixel photosynthetic activity (indicated by REP) and atmospheric drought stress (indicated by VPD), distinguish between estuarine and marine mangroves, and aggregate them into half-degree cells to construct two coupling metrics. Subsequently, climate zone types, salinity, and rainfall data were introduced to further investigate the regional differences in coupling among different climate zones, as well as the impact of salinity and hydrological environment on the coupling. We hypothesize that (1) a significant coupling exists between mangrove photosynthetic activity and atmospheric drought stress, and (2) this coupling is stronger in marine mangroves experiencing a higher salinity stress than in estuarine mangroves experiencing a lower salinity stress. We aim to answer the following scientific questions: (1) How is the coupling between mangrove photosynthetic activity and atmospheric drought stress? (2) What are the spatial differences in the coupling regarding various climate zones and mangrove habitats (i.e., marine vs. estuarine)?

2. Data and methods

The technical roadmap of this study is shown in Fig. 2.

2.1. Mangrove distributions and environmental data

This study used a grid cell with a spatial resolution of 0.5° in the data analyses. Firstly, seamless global grid cells with a resolution of 0.5° (approximately 50 km at the equator) were established. Secondly, the global spatial distribution of mangroves with a resolution of 10 m from the HGMF_2020 dataset (Jia et al., 2023) was used to identify the presence of mangroves, forming 3033 grid cells with a resolution of 0.5°. These cells were distributed between 39°S and 30°N, covering all longitudinal bands. Thirdly, since marine and estuarine mangroves have distinct habitats and face different threats (Kimirei et al., 2016), we classified estuarine and marine mangroves within each grid cell. Some cells have both marine mangroves and estuarine mangroves, while others only have one type of mangrove. The global estuary distribution mask developed by the "Sea Around Us" project (Alder, 2003) was applied to the mangrove distribution dataset to distinguish between marine and estuarine mangroves. To avoid missing mangroves around estuarine areas, a 5-km buffer zone was established for the estuarine mask. Among all grid cells, marine mangroves exist in 2879 cells, and estuarine mangroves exist in 766 cells. For subsequent analyses, each grid cell was assigned two types of attributes: mangrove attributes and environmental attributes. Cell-level mangrove attributes were calculated from all mangrove pixels within the grid cell, while cell-level environmental attributes, including climatic zone, seawater salinity, and annual rainfall, were calculated from all pixels within the grid cell.

Temperature has already been considered the main limiting factor for the geographical distribution of mangrove forests (Saintilan et al., 2014). Mangrove forests are extremely sensitive to temperature changes, and extreme high and low temperatures can affect their growth (Duke et al., 2017; Giri et al., 2011). Therefore, the photosynthetic activity of mangroves in different latitudinal zones and climate zones is expected to respond differently to drought stress. The global map of the Köppen-Geiger climate classification for the period 1991–2020 with a resolution of 0.5° was available from GloH2O (Beck et al., 2023). According to the Köppen-Geiger classification criteria (Yoo & Rohli, 2016), the land climate in the distribution area of mangrove forests consisted of

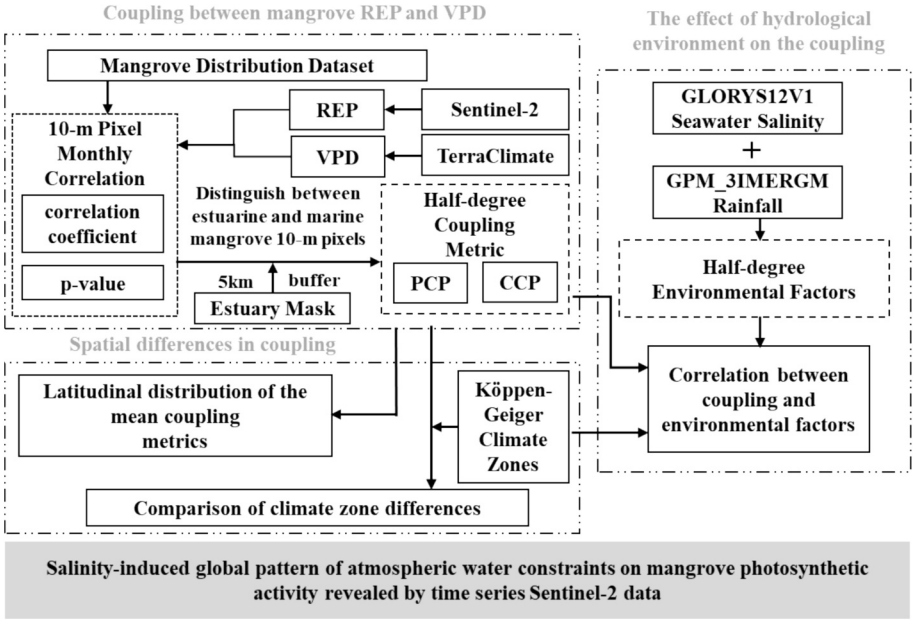

Fig. 2. Workflow of analysis of spatial differences in the coupling between mangrove photosynthetic activity and atmospheric drought stress.

three main types, with tropical regions being larger and further subdivided into three subtypes. All grid cells had a total of 5 climate types, including tropical rainforest climate (Af), tropical monsoon climate (Am), tropical savanna climate (Aw), desert and semi-arid climate (B), and temperate climate (C) (Fig. A1a).

High salinity is a major limiting factor for mangrove growth and photosynthesis, which is expected to weaken the adaptability of mangroves to drought stress. However, the salt mass balance of mangrove systems is influenced by various factors, such as large-scale ocean circulation, river water input, and precipitation (Gomez et al., 2019; Lane et al., 2007). Given the complexity and difficulty of measuring actual porewater salinity, seawater salinity is used as a reasonable proxy in this study, like previous studies (Kirwan et al., 2009; McKee, 2011; Simard et al., 2019). The monthly seawater salinity was sourced from the GLORYS12V1 product provided by the Copernicus Ocean Service (Lellouche et al., 2021), with a spatial resolution of 0.083°. The average monthly seawater salinity during the research period was used for subsequent analyses (Fig. A1b). Adequate rainfall is crucial for diluting porewater salinity and maintaining a healthy mangrove ecosystem. The increase in rainfall can also lead to a decrease in porewater salinity and sulfate concentration, thereby enhancing the photosynthetic activity of mangroves (Ward et al., 2016; Zhu, Sun, & Qin, 2021). The GPM_3IMERGM product with a spatial resolution of 0.1° from the NASA Global Precipitation Measurement Mission (Huffman et al., 2023) provided the monthly rainfall data to calculate the mean annual rainfall (Fig. A1c).

2.2. Mangrove REP and its coupling with VPD

The coupling analyses based on long-term spatiotemporal data were implemented with the Google Earth Engine (GEE) platform. As the "COPERNICUS/S2_SR_HARMONIZED" dataset for the Sentinel-2 Level 2A product has only provided complete global coverage data since 2019, the time range of this study was from 2019 to 2023. VPD is widely recognized as a proxy for atmospheric drought stress due to its direct influence on plant physiological processes (Zhang et al., 2024). We used the TerraClimate dataset to obtain global VPD data, a high-resolution (~4-km, 1/24°) global monthly climate dataset (Abatzoglou et al., 2018). Among the variables provided by TerraClimate, we directly extracted monthly VPD values.

The REP, used for representing mangrove photosynthetic activity, was calculated from Sentinel-2 surface reflectance data (Level 2A products). To improve data quality, we used the Cloud Score Plus (CSP) cloud detection algorithm to estimate the cloud probability of each pixel (Pasquarella et al., 2023). On the GEE platform, the "Cloud Score + S2-HRMONIZE V1″ dataset provides a standard for the CSP algorithm, where the "CS" band represents cloud probability and the "CS_CDF" band represents the CS band's cumulative distribution function (CDF). This study used the "CS_CDF" band to identify pixels blocked by clouds and used 0.6 as a threshold to remove pixels larger than the threshold (Hang et al., 2024). Due to the discontinuity of spectral reflectance in satellite data, the four-point linear interpolation method was used to estimate REP (Clevers et al., 2002). This method assumes that the reflectance curve of the red-edge band can be approximated as a straight line with REP as the midpoint between the near-infrared band (780 nm) and the red band (670 nm) (Gholizadeh et al., 2016):

$$\mathrm{REP} = 700 + 40 \times \left(\frac{\frac{R_{670}+R_{780}}{2} - R_{700}}{R_{740} - R_{700}} \right) \quad (1)$$

According to the center wavelength of the relevant band of Sentinel-2, it can be rewritten as:

$$\mathrm{REP} = 704 + 36 \times \left(\frac{\frac{R_{665}+R_{780}}{2} - R_{704}}{R_{740} - R_{704}} \right) \quad (2)$$

where R_{665}, R_{704}, R_{740}, R_{780} are the reflectance values at 665, 704, 740 and 780 nm, respectively.

To avoid outlier interference, the monthly REP was calculated as the median of all available images for that month. For each 10-m mangrove pixel, the Pearson correlation coefficient and significance test were performed on the monthly REP and VPD time series to determine the coupling between the two variables. Each pixel has a correlation coefficient and a p-value. However, for the half-degree grid cells, two coupling metrics were defined as follows: (1) PCP: the proportion of coupling 10-m mangrove pixels with statistically significant REP-VPD correlations ($p < 0.05$) in the total number of mangrove pixels within the half-degree cell; (2) CCP: the median correlation coefficient of coupling 10-m mangrove pixels with statistically significant REP-VPD correlations within the half-degree cell.

2.3. Data analyses

We analyzed the correlation between the coupling metrics and their spatial location characteristics (e.g., geographical location and environmental conditions). To better explore the regular changes in the distribution of mangrove forests from the southern edge to the northern edge, all half-degree grid cells were grouped equally at an interval of 1° according to latitude (Perri et al., 2023), resulting in 70 sets of mangrove attributes for examining the relationship between coupling and latitudinal zones. Regression analyses were conducted between the coupling of half-degree grid cells and environmental factors. We selected two environmental factors (i.e., seawater salinity and annual rainfall), with the PCP representing the coupling for analysis. During the fitting process, all half-degree grid cells were divided into 10 groups proportionally based on environmental factors, and the average values were used for regression analyses. Both linear and exponential responding functions were tested in the regression analyses, but only one type of the function with better performance was applied in the further analyses to describe the impacts of changing seawater salinity and annual rainfall on the PCP.

In addition, the quality and quantity of river inputs and large-scale ocean circulation can affect the salt balance of mangrove ecosystems, so mangroves in marine and estuarine habitats were classified (Gomez et al., 2019; Lane et al., 2007). Thus, for all half-degree grid cells, we calculated three types of coupling indicators, namely marine mangrove coupling, estuarine mangrove coupling, and total mangrove coupling, and then compared the impact of differences in marine and estuarine habitats on coupling under the same spatial location conditions. The Mann-Whitney U test (Vierra et al., 2023) was used to detect the coupling differences between marine and estuarine mangroves. Each half-degree grid cell was directly assigned to one of the five climate zones. We compared the coupling of these five groups of half-degree grid cells to examine the impact of climate zones. We also analyzed differential responses of the coupling to increasing seawater salinity and annual rainfall for five climatic zones between marine and estuarine mangrove habitats.

3. Results

3.1. Coupling between mangrove REP and VPD

From 2019 to 2023, the coupling between mangrove photosynthetic activity and atmospheric drought stress was generally good on a global scale. In terms of PCP, the median value of all half-degree grid cells was 0.41 (mean: 0.38), and there were 1376 cells (out of 3033 cells) with a PCP > 0.5. Geographically, the PCP in the Caribbean region of Central America, the Malay Archipelago region, the coast of Australia, and the eastern side of the Mozambique Channel could reach 0.8 or above (Fig. 3a). The PCP distribution exhibited substantial spatial variability. For all half-degree grid cells, 83% of them had negative correlation coefficients, illustrating that mangrove photosynthetic activity generally

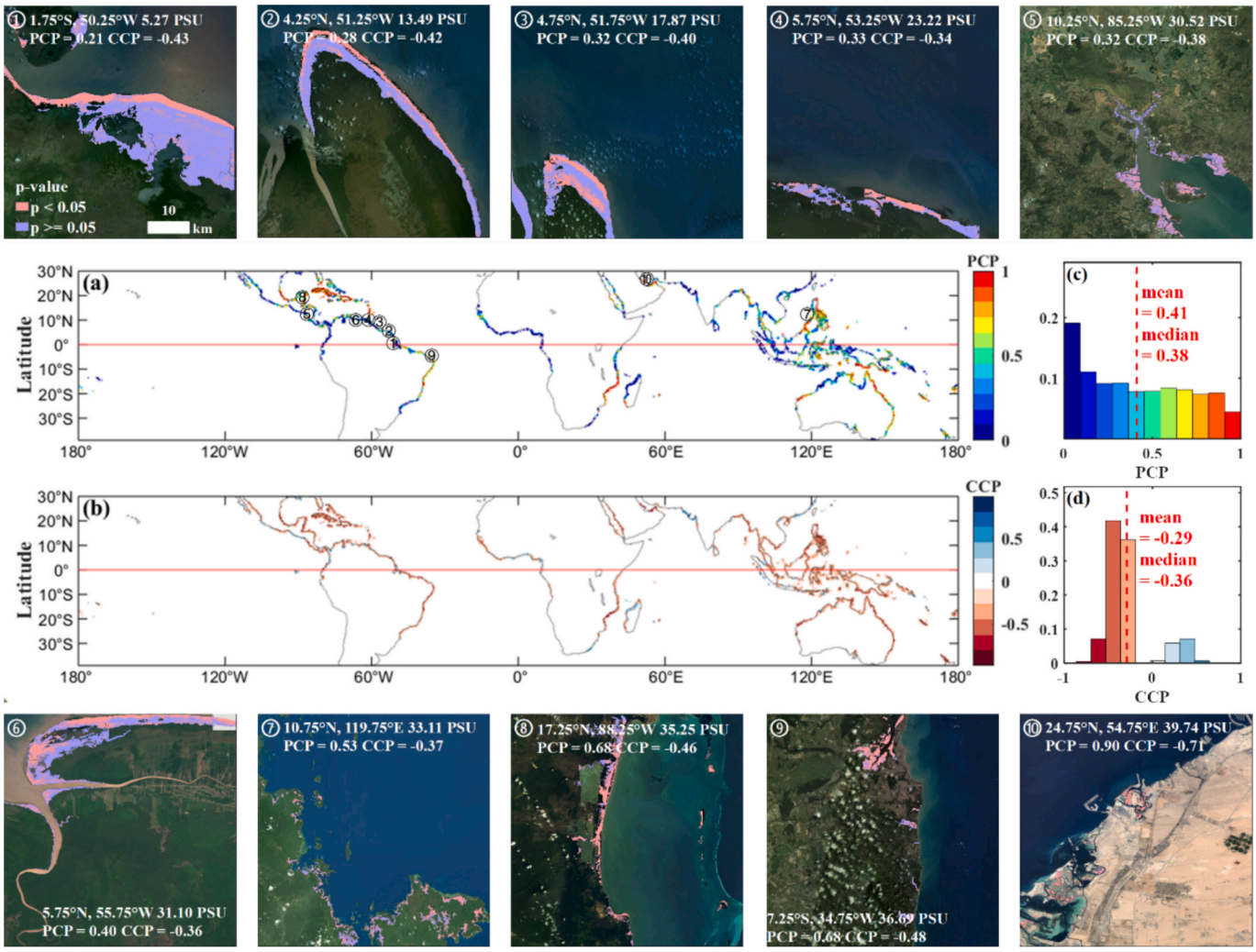

Fig. 3. Global mappings (a and b) and corresponding statistical distributions (c and d) of the coupling metrics, PCP (proportion of coupling 10-m mangrove pixels) and CCP (median correlation coefficient of coupling 10-m mangrove pixels), for all half-degree grid cells covering 10-m mangrove pixels. Subfigures ① to ⑩ (seawater salinity from low to high) represent the correlation significance of 10-m mangrove pixels within a grid cell. The positions of these grid cells are marked.

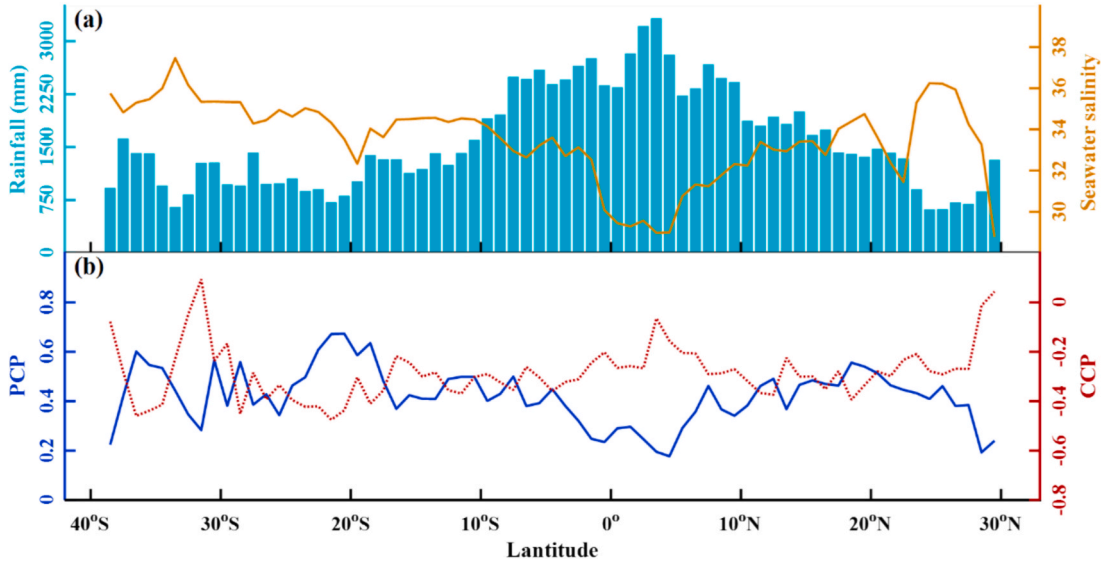

Fig. 4. Latitudinal distribution of mean seawater salinity and rainfall (a) and the mean coupling metrics (b), PCP (proportion of coupling 10-m mangrove pixels) and CCP (median correlation coefficient of coupling 10-m mangrove pixels), within the mangrove distribution range from 39°S to 30°N.

decreased with increasing atmospheric drought stress. The global median CCP was −0.29 (mean: −0.36), and more than half of the grid cells varied between −0.3 and −0.5, with no significant spatial difference compared to PCP (Fig. 3b). When the data were analyzed separately for marine and estuarine mangroves, we found that marine mangroves had larger PCP (mean: 0.42 vs. 0.34; median: 0.40 vs. 0.26) and stronger CCP (mean: −0.30 vs. −0.23; median: −0.36 vs. −0.34) than estuarine mangroves (Fig. A2-3). When 10 cells with different salinity levels were selected from all global grid cells, it was evident that as salinity increased, the value of PCP also increased. Within each cell, there were significantly more pixels with a significant negative correlation between REP and VPD near the coast (Fig. 3).

3.2. Spatial differences in coupling between REP and VPD

From the southern to the northern edge of the geographical distribution range of mangrove forests, the seawater salinity first decreased and then increased, reaching its minimum value near the equator (Fig. 4). Rainfall had an opposite latitudinal trend, reaching a maximum annual rainfall of 3321 mm in the 3°N zone. PCP and CCP had opposite latitudinal trends, indicating that the higher the PCP, the stronger the negative correlation between photosynthetic activity and atmospheric drought stress (i.e., the stronger the coupling). Overall, the latitudinal variation patterns of these coupling metrics and salinity/rainfall were consistent. Taking the 5°S-5°N zone for example, low salinity (or high rainfall) well corresponded to weak coupling (i.e., low PCP and weak CCP). Over the whole latitudinal zone, the weakest coupling occurred in the 4°N zone (mean PCP = 0.18), while the strongest coupling occurred in the 21°S zone (mean PCP = 0.67).

For the differences between marine and estuarine mangrove forests, both PCP and CCP passed the Mann-Whitney *U* test, indicating a statistically significant difference in the coupling between marine and estuarine habitats (Fig. 5). For the differences among climate zones, the highest median PCP (0.43) occurred in the tropical savanna climate zone, while the lowest median PCP (0.32) occurred in the temperate climate zone. The strongest value of the median CCP was −0.37 in the tropical savanna climate zone, while the weakest value was −0.34 in the tropical rainforest climate zone.

3.3. The effect of hydrological environment on the coupling

To further analyze regional differences, the coupling metric of PCP was used for analyses of the effects of environmental factors. For marine habitats (Fig. 6a-f), as the salinity of the sea surface increased, the coupling rapidly increased, and the growth rate increased faster with the increase of salinity, following the expression of an exponential function ($y = a \times e^{bx/10}$). In all climate zones where mangroves grow, the coupling increased exponentially with salinity, and the determination coefficients of the fitted equations were all greater than 0.5. Comparing the parameter b in the equation expression, the maximum value was 3.09 for climate zone C, while the minimum value was 0.80 for climate zone Am. For estuarine habitats (Fig. 6g-l), similar responding patterns were found. The parameter b showed a maximum value of 2.52 in climate zone C and a minimum value of 1.89 in climate zone Am. However, in estuarine habitats, we also observed a low determination coefficient of 0.16 in climate zone B, with a relatively narrow range of salinity variation (Fig. 6j).

As annual rainfall increased, the coupling tended to decrease uniformly following the expression of a linear function ($y = ax + b$) (Fig. 7). For marine habitats (Fig. 7a-f), except for the Aw climate zone, the determination coefficients of the fitted equations were greater than 0.5. Among the five climate zones, climate zone B had the highest slope

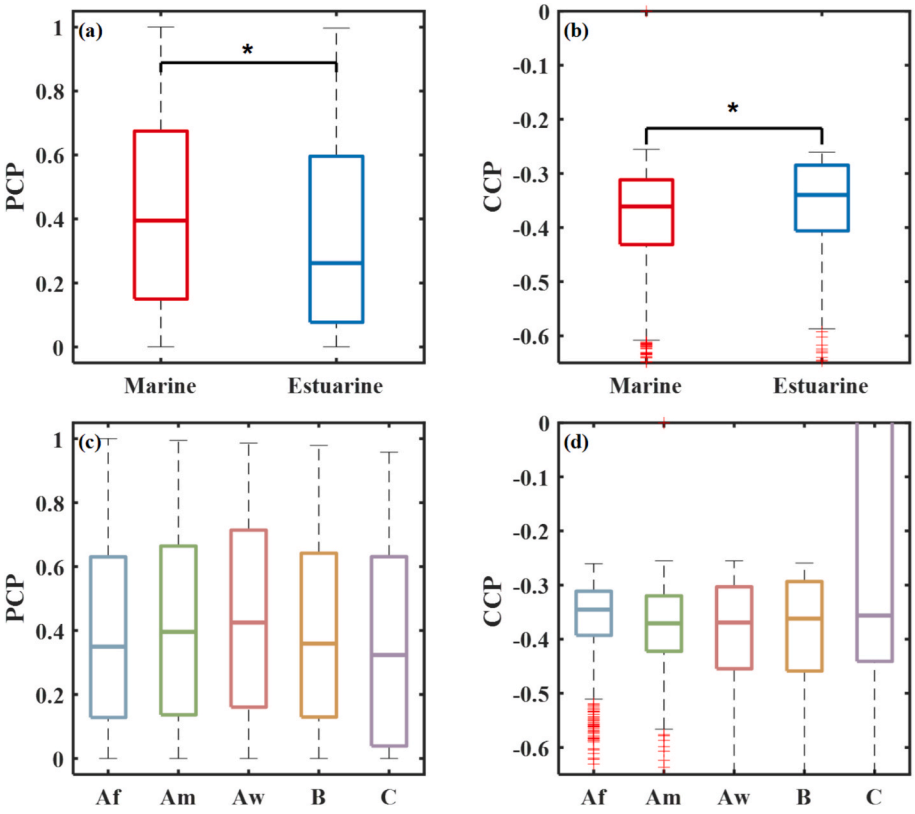

Fig. 5. Comparisons of the coupling metrics, PCP (proportion of coupling 10-m mangrove pixels) and CCP (median correlation coefficient of coupling 10-m mangrove pixels), between marine and estuarine mangroves (a and b) ("*" represents a statistically significance of $p < 0.05$) and among five climate zones (c and d) including tropical rainforest climate (Af), tropical monsoon climate (Am), tropical savanna climate (Aw), desert and semi-arid climate (B), and temperate climate (C).

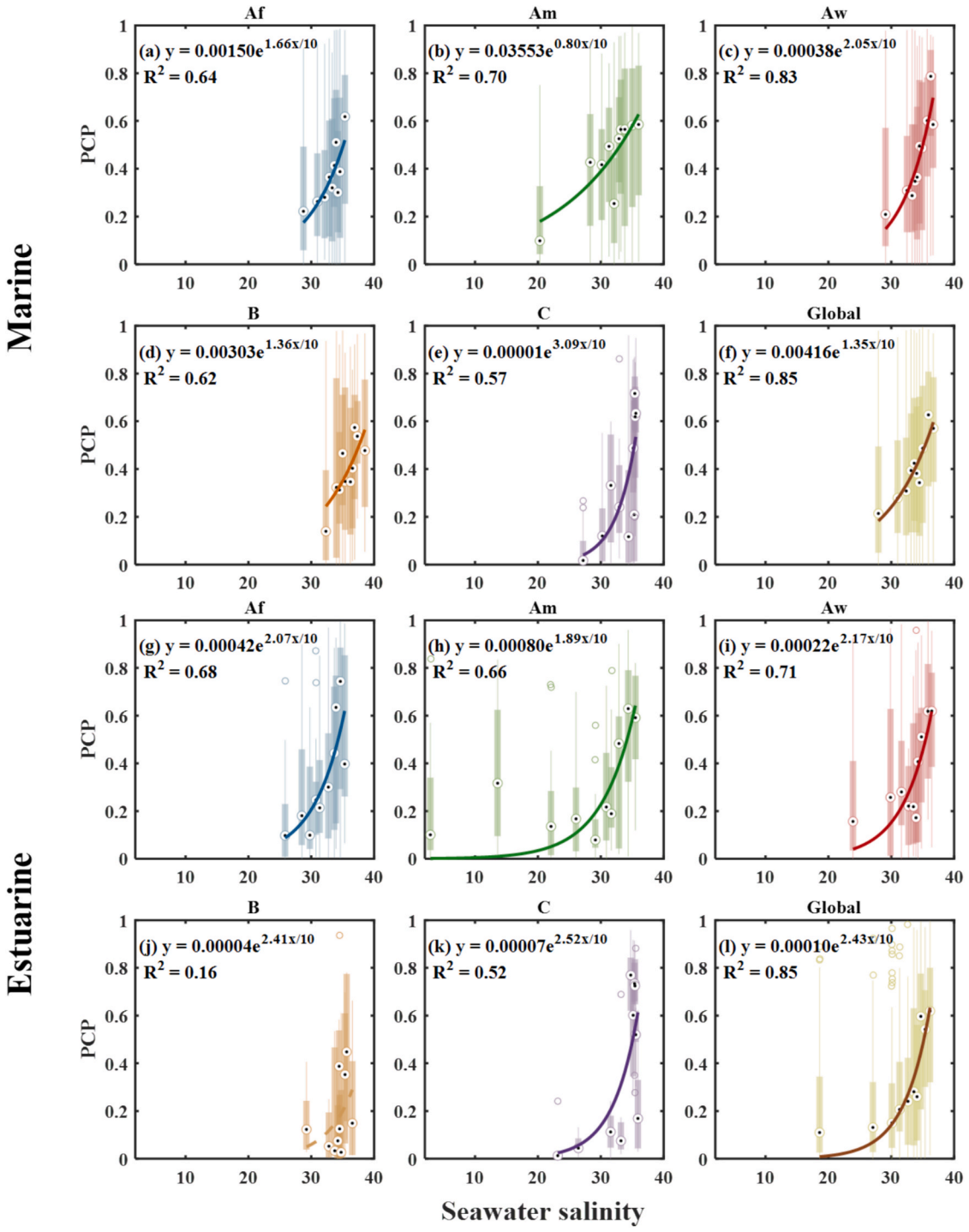

Fig. 6. Differential response of the coupling metric of PCP (proportion of coupling 10-m mangrove pixels) to increasing seawater salinity for global and five different climatic zones between marine (upper panel) and estuarine (lower panel) mangrove habitats. Climatic zones include tropical rainforest climate (Af), tropical monsoon climate (Am), tropical savanna climate (Aw), desert and semi-arid climate (B), and temperate climate (C). Data from all half-degree grid cells were equally divided into ten groups (percentile-based), and then the median values of each group were used for exponential regressions. Solid and dashed fitting curves indicate statistically ($p < 0.05$) significant and non-significant.

of −0.50, while climate zone Am had the lowest slope of −0.10. For estuarine habitats (Fig. 7g-l), this linear relationship was not as pronounced as in marine habitats. This relationship was not statistically significant in two climate zones (Aw and C), and the coefficient of determination was generally weaker than that in marine habitats. The differences between climate zones were similar when the analyses were conducted based on all mangrove forests from marine and estuarine habitats (Fig. A4-5).

4. Discussion

4.1. Atmospheric water constraints on mangrove photosynthetic activity

On a monthly scale, the coupling between atmospheric drought stress and photosynthetic activity reflects the atmospheric water constraints on mangrove photosynthetic activity. Consistent with terrestrial forests, the intensification of atmospheric drought stress, characterized

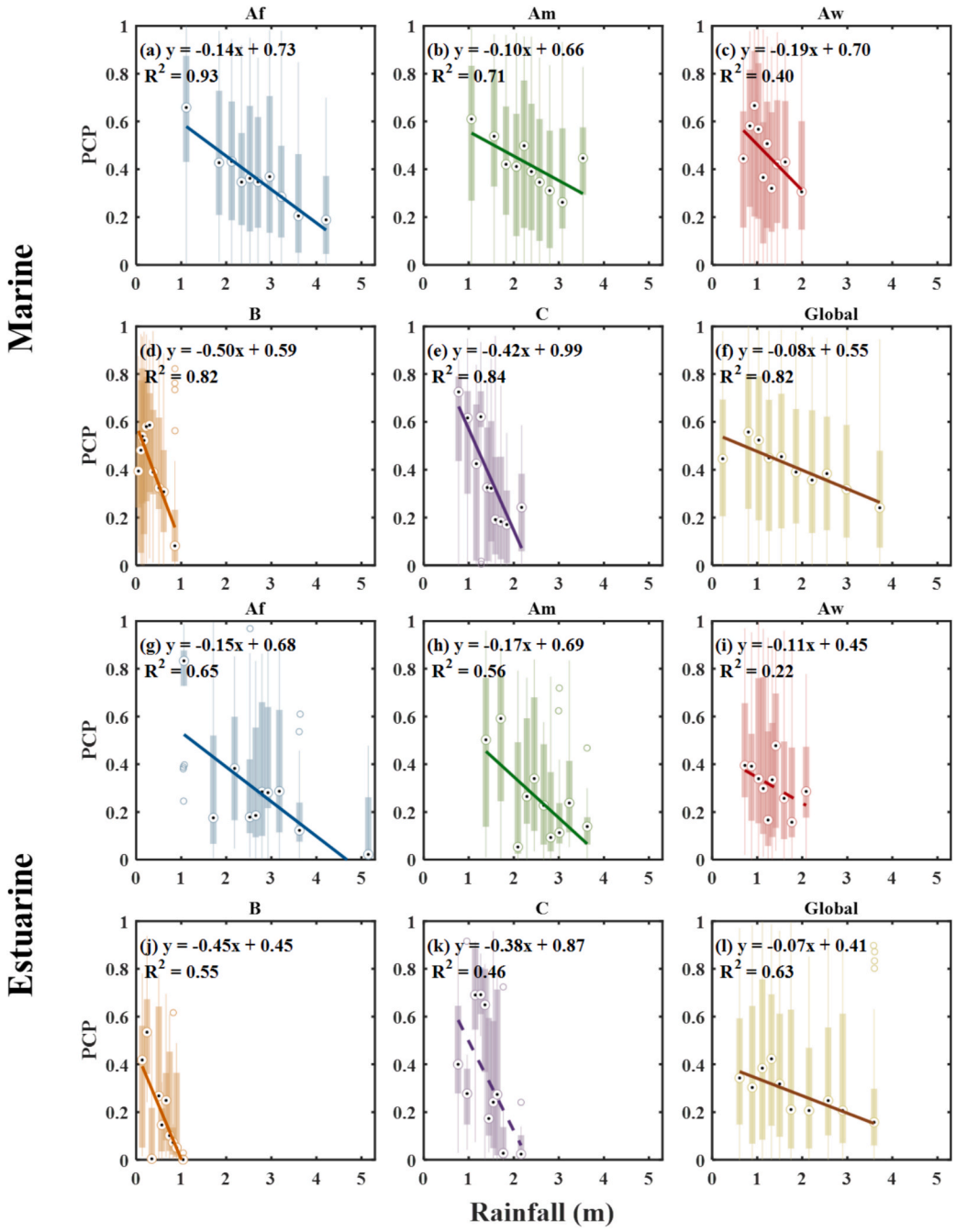

Fig. 7. Differential response of the coupling metric of PCP (proportion of coupling 10-m mangrove pixels) to increasing annual rainfall for global and five different climatic zones between marine (upper panel) and estuarine (lower panel) mangrove habitats. Climatic zones include tropical rainforest climate (Af), tropical monsoon climate (Am), tropical savanna climate (Aw), desert and semi-arid climate (B), and temperate climate (C). Data from all half-degree grid cells were equally divided into ten groups (percentile-based), and then the median values of each group were used for linear regressions. Solid and dashed fitting curves indicate statistically ($p < 0.05$) significant and non-significant.

by increases in VPD, has been widely reported as an important abiotic environmental factor that reduces the photosynthetic capacity of mangroves (Alvarado-Barrientos et al., 2021; Gnanamoorthy et al., 2020; Leopold et al., 2016; Zhao et al., 2022). In response to increasing atmospheric dryness, mangroves decrease stomatal conductance to reduce water loss, thereby affecting CO_2 uptake through photosynthesis (Jiang et al., 2017; Keith et al., 2012). Existing site observations have found that mangroves located in diverse climatic regions exhibit a decrease in photosynthetic activity during periods of high temperature and high VPD (Gnanamoorthy et al., 2020; Rodda et al., 2022). Our findings provide strong empirical evidence that atmospheric water constraints on mangrove photosynthetic activity represent a globally pervasive phenomenon, rather than a regionally confined or species-specific anomaly (Figs. 3a and A2-3). Across a wide range of climate zones and latitudinal gradients, mangroves consistently exhibit the blue-shift phenomenon of REP during high-VPD seasons. These responses have been documented in tropical, subtropical, and even marginal poleward populations, suggesting that atmospheric dryness is a universal stressor shaping mangrove photosynthesis at the global scale (Bardou et al., 2024; Lovelock et al., 2016; Yuan et al., 2019). Thus, atmospheric water constraints on mangrove photosynthesis should be viewed as a core and globally relevant physiological limitation, embedded within a broader

framework of hydroclimatic sensitivity.

Although atmospheric drought stress commonly inhibits mangrove photosynthetic activity worldwide, spatial heterogeneity in environmental conditions results in a wide spectrum of physiological adaptations and responses across regions. While mangroves generally demonstrate greater tolerance to elevated VPD compared to many terrestrial ecosystems due to their conservative water-use strategies (Li et al., 2025), our results highlight substantial intra-biome variability. In tropical rainforest climate zones near the equator, high annual rainfall and persistent humidity keep atmospheric water demand low, leading to minimal VPD-induced stress responses (Fig. 4b and 5c-d). Under humid conditions, water availability rarely limits gas exchange, allowing mangrove canopies to maintain high stomatal conductance and photosynthetic activity throughout the year (Dali, 2023). Equatorial mangroves benefit from abundant rainfall that promotes sustained growth and carbon uptake, with atmospheric water constraints playing a relatively minor role compared to light or nutrient limitations (Krauss et al., 2022). This favorable moisture regime means that photosynthetic performance in equatorial mangrove forests is primarily constrained by factors such as light and nutrients rather than atmospheric dryness (Mwangi et al., 2001). In contrast, mangroves in tropical savanna climate zones experience pronounced rainfall seasonality, which intensifies atmospheric water limitations during dry periods. High temperatures and clear skies during the dry season drive up VPD (Cai et al., 2023), and these seasonal droughts force mangroves to adopt conservative water-use strategies. To cope, subtropical mangroves enhance water-use efficiency through osmotic adjustment, reduced canopy conductance, and tighter stomatal control strategies that allow limited photosynthetic activity under stress (Li et al., 2025). As a result, a strong seasonal coupling emerges between VPD fluctuations and photosynthetic performance in these regions, as reflected in our spatial analyses (Fig. 4b and 5c-d). Our analyses showed that mangroves in temperate climate zones (i.e., subtropical areas) did not exhibit a strong seasonal negative correlation between photosynthetic activity and atmospheric dryness. This does not mean that atmospheric water stress is no longer the primary source of growth pressure for mangrove forests at the northern and southern distributional edges. In subtropical regions, the interplay between VPD and photosynthesis is modulated by factors such as soil salinity, light intensity, temperature, and nutrient availability (Yoshikai et al., 2022; Zheng & Takeuchi, 2022). These factors can attenuate the negative correlation between VPD and photosynthetic activity.

4.2. Salinity-induced global pattern of atmospheric water constraints

Mangrove photosynthesis is shaped not only by atmospheric water demand but also by salinity stress, which serves as a critical regulator of plant water uptake across diverse climatic and hydrological settings. Elevated salinity increases the osmotic potential of soil water, making it more difficult for mangrove roots to extract water, thereby effectively intensifying physiological drought even when atmospheric humidity remains moderate (Kimera et al., 2024; Parida & Jha, 2010). This osmotic stress leads to partial or complete stomatal closure to reduce water loss, thereby lowering internal CO_2 concentrations and constraining photosynthetic carbon assimilation (Li et al., 2022). Additionally, energy allocated to ion exclusion, compartmentalization, or the synthesis of compatible solutes such as proline or glycine betaine under saline conditions further reduces photosynthetic efficiency by diverting resources away from carbon fixation pathways (Chakraborty et al., 2018). The limiting effect of salinity on PCP follows an exponential relationship, and during the initial stages of salinity increase, no significant difference is observed in atmospheric water constraints on mangrove photosynthetic activity (Fig. 6). As halophytic species, mangroves require a certain salinity range for optimal physiological functioning, and moderate salinity levels can even enhance photosynthetic activity (Roose et al., 2016). For example, Gnanamoorthy et al. (2020) reported that salinity conditions of 3–25 PSU promote mangrove productivity in the Indian tropical mangrove forest of Pichavaram. Rainfall is widely employed as a proxy indicator of salinity regimes in mangrove ecosystems because freshwater inputs from rainfall and river discharge directly regulate porewater salinity (Alongi, 2015; Wahid et al., 2025). In regions characterized by frequent or abundant rainfall, dilution of seawater by freshwater inputs alleviates salinity stress and permits higher stomatal conductance, thereby buffering mangroves against atmospheric drought stress (Fig. 7).

In tropical monsoon climate zones, where rainfall exhibits pronounced seasonality, mangrove species are commonly adapted to alternating wet and dry phases with corresponding salinity variability, which does not necessarily intensify atmospheric drought stress effects unless freshwater limitation persists over extended periods (Figs. 6b and 7b). During the wet season, salinity is generally diluted, alleviating osmotic stress and enhancing gas exchange capacity even when VPD increases in response to higher temperatures (Friess et al., 2022). During the dry season, while both VPD and salinity rise, mangroves in monsoon regions often exhibit acclimation strategies such as enhanced water-use efficiency and reduced leaf area to mitigate stress (Cheeseman, 2015; Krauss et al., 2008). Consequently, atmospheric water constraints may respond less strongly to increasing salinity in these zones because of species-specific physiological plasticity and seasonally mediated buffering effects.

4.3. Limitations and uncertainties

There are certain limitations and uncertainties in our analyses of the minimum cell based on Sentinel-2 data and other open-source spatiotemporal data sets at a resolution of 0.5°. Firstly, the datasets we use have a certain degree of uncertainty. Due to the discontinuity of satellite bands, we can only use adjacent bands to calculate REP, ignoring the nonlinear characteristics that exist in the red-edge band (Li et al., 2024). When calculating the monthly REP, directly deleting pixels blocked by clouds may result in the loss of some information (Arp et al., 2024), but for the original Sentinel-2 imagery, we only removed those images that were obscured by clouds and did not restore a continuous spatiotemporal sequence. However, many mangrove forests are distributed in cloudy areas throughout the year, and we may have lost some information. The spatial resolution of the TerraClimate dataset is 4 km; therefore, it cannot record finer spatial variations in VPD. Seawater salinity is considered a proxy for porewater salinity, but due to the complexity of the environment, its value is often lower than the true porewater salinity, so this proxy is relatively conservative. Secondly, our analysis process has limitations. A 0.5° grid cell might cause us to lose more detailed information, especially when it comes to environmental factors, as we overlook their rapid spatial variability (Habib et al., 2008). When discussing the coupling between photosynthetic activity and atmospheric drought stress, we did not take the possible hysteresis response between the two into account. In the future, more statistical methods need to be applied to quantify potential asynchrony between the two (Knox et al., 2021). Finally, the impact of species diversity and interspecific differences had not been discussed, and the richness of mangrove ecosystems is likely to also affect the sensitivity of photosynthetic activity to stress (Gatti et al., 2017). In addition, when summarizing regional differences, we lack consideration for other environmental driving forces, such as sea level rise and regional differences in tropical cyclones (Krauss et al., 2008), which also have important impacts on the photosynthetic activity of mangrove ecosystems.

5. Conclusion

Based on Sentinel-2 satellite data from 2019 to 2023 and open-source meteorological environment spatiotemporal data, we studied the coupling between global mangrove red-edge position and VPD on a

seasonal scale to explore atmospheric water constraints on mangrove photosynthetic activity. Our results demonstrate a consistent global decrease in photosynthetic activity under increasing atmospheric drought. When the atmosphere becomes drier, the photosynthesis of mangroves is weaker, but their sensitivity to drought stress exhibits significant spatial variations. From the perspective of climate zones, tropical rainforest regions have not yet experienced significant drought stress, but the photosynthesis of mangrove forests in tropical savanna climate regions is significantly weakened under drought stress. From the perspective of the hydrological environment, salinity stress intensifies the sensitivity of photosynthetic activity to atmospheric drought stress, and mangrove forests in marine habitats are more sensitive to drought stress due to long-term exposure to high salt environments. Mangrove forests in tropical savanna climates and high-salinity habitats should therefore be prioritized for conservation due to their heightened vulnerability.

CRediT authorship contribution statement

Yanjie Liu: Writing – original draft, Visualization, Investigation, Formal analysis, Data curation. **Yueting Deng:** Writing – review & editing, Methodology, Investigation, Formal analysis. **Hui Luo:** Writing – review & editing, Visualization, Software, Formal analysis, Data curation. **Nengwang Chen:** Visualization, Methodology, Formal analysis, Conceptualization. **Yougan Chen:** Visualization, Software, Formal analysis, Data curation. **Zhenong Jin:** Writing – review & editing, Software, Methodology, Formal analysis. **Xu Wang:** Writing – review & editing, Visualization, Software, Conceptualization. **Hongsheng Zhang:** Writing – review & editing, Software, Methodology, Conceptualization. **Xudong Zhu:** Writing – review & editing, Supervision, Project administration, Methodology, Investigation, Funding acquisition, Formal analysis, Data curation, Conceptualization.

Declaration of competing interest

The authors declare that they have no known competing financial interests or personal relationships that could have appeared to influence the work reported in this paper.

Acknowledgments

This work was jointly supported by the National Key Research and Development Program of China (2022YFF0802101, 2024YFF1306805), Natural Science Foundation of Fujian Province of China (2023J06008), the National Natural Science Foundation of China (32371661), Shenzhen Science and Technology Plan Project (KCXST20221021111404011), the 2023 Google Carbon Removal Research Awards, and the 2024 Google Climate Action Student Research Grants (China) (PJ240068). The authors also thank Chenjuan Zheng for her help on the data processing.

Appendix A. Supplementary data

Supplementary data to this article can be found online at https://doi.org/10.1016/j.jag.2026.105170.

Data availability

The data that supports the findings of this study are available in the supplementary material of this article.

References

Abatzoglou, J.T., Dobrowski, S.Z., Parks, S.A., et al., 2018. TerraClimate, a high-resolution global dataset of monthly climate and climatic water balance from 1958-2015. Sci. Data 5 (1), 170191. https://doi.org/10.1038/sdata.2017.191.

Alder, J., 2003. Putting the coast in the "Sea around Us". The Sea around Us Newsletter 15, 1–2. http://seaaroundus.org/newsletter/Issue15.pdf.

Alongi, D., 2009. The energetics of mangrove forests. Springer Science & Business Media. https://doi.org/10.1007/978-1-4020-4271-3.

Alongi, D.M., 2015. The impact of climate change on mangrove forests. Current Climate Change Reports 1 (1), 30–39. https://doi.org/10.1007/s40641-015-0002-x.

Alvarado-Barrientos, M.S., López-Adame, H., Lazcano-Hernández, H.E., et al., 2021. Ecosystem-atmosphere exchange of CO_2, water, and energy in a basin mangrove of the northeastern coast of the Yucatan Peninsula. J. Geophys. Res. Biogeo. 126 (2), e2020JG005811. https://doi.org/10.1029/2020JG005811.

Arp, L., Hoos, H., Van Bodegom, P., et al., 2024. Training-free thick cloud removal for Sentinel-2 imagery using value propagation interpolation. ISPRS J. Photogramm. Remote Sens. 216, 168–184. https://doi.org/10.1016/j.isprsjprs.2024.07.030.

Bardou, R., Pullen, J., Cavanaugh, K.C., et al., 2024. Effects of cold water and aridity on Baja California mangrove survival and ecophysiological traits. J. Ecol. 112 (5), 985–997. https://doi.org/10.1111/1365-2745.14264.

Beck, H.E., Mcvicar, T.R., Vergopolan, N., et al., 2023. High-resolution (1 km) Köppen-Geiger maps for 1901-2099 based on constrained CMIP6 projections. Sci. Data 10 (1), 72. https://doi.org/10.1038/s41597-023-02549-6.

Cai, G., Wankmüller, F., Ahmed, M.A., et al., 2023. How the interactions between atmospheric and soil drought affect the functionality of plant hydraulics. Plant Cell Environ. 46 (3), 733–735. https://doi.org/10.1111/pce.14538.

Chakraborty, K., Basak, N., Bhaduri, D., et al., 2018. Ionic basis of salt tolerance in plants: Nutrient homeostasis and oxidative stress tolerance. Plant Nutrients and Abiotic Stress Tolerance 325–362. https://doi.org/10.1007/978-981-10-9044-8_14.

Cheeseman, J.M., 2015. The evolution of halophytes, glycophytes and crops, and its implications for food security under saline conditions. New Phytol. 206 (2), 557–570. https://doi.org/10.1111/nph.13217.

Chung, C.T., Hope, P., Hutley, L.B., et al., 2023. Future climate change will increase risk to mangrove health in Northern Australia. Commun. Earth Environ. 4 (1), 192. https://doi.org/10.1038/s43247-023-00852-z.

Clevers, J.G.P.W., De Jong, S.M., Epema, G.F., et al., 2002. Derivation of the red edge index using the MERIS standard band setting. Int. J. Remote Sens. 23 (16), 3169–3184. https://doi.org/10.1080/01431160110104647.

Cotovicz Jr, L., Abril, G., Sanders, C., et al., 2024. Methane oxidation minimizes emissions and offsets to carbon burial in mangroves. Nat. Clim. Chang. 14, 1–7. https://doi.org/10.1038/s41558-024-01927-1.

Croft, H., Chen, J.M., Luo, X., et al., 2017. Leaf chlorophyll content as a proxy for leaf photosynthetic capacity. Glob. Chang. Biol. 23 (9), 3513–3524. https://doi.org/10.1111/gcb.13599.

Cui, X., Liang, J., Lu, W., et al., 2018. Stronger ecosystem carbon sequestration potential of mangrove wetlands with respect to terrestrial forests in subtropical China. Agric. For. Meteorol. 249, 71–80. https://doi.org/10.1016/j.agrformet.2017.11.019.

Dali, G.L.A., 2023. Litter production in two mangrove forests along the coast of Ghana. Heliyon 9 (6), e17004. https://doi.org/10.1016/j.heliyon.2023.e17004.

Donato, D.C., Kauffman, J.B., Murdiyarso, D., et al., 2011. Mangroves among the most carbon-rich forests in the tropics. Nat. Geosci. 4 (5), 293–297. https://doi.org/10.1038/ngeo1123.

Duarte, C.M., Losada, I.J., Hendriks, I.E., et al., 2013. The role of coastal plant communities for climate change mitigation and adaptation. Nat. Clim. Chang. 3 (11), 961–968. https://doi.org/10.1038/nclimate1970.

Duke, N.C., Kovacs, J.M., Griffiths, A.D., et al., 2017. Large-scale dieback of mangroves in Australia's Gulf of Carpentaria: a severe ecosystem response, coincidental with an unusually extreme weather event. Mar. Freshw. Res. 68 (10), 1816–1829. https://doi.org/10.1071/MF16322.

Friess, D., Adame, F., Adams, J., et al., 2022. Mangrove forests under climate change in a 2°C world. WIREs Clim. Change 13 (4), e792.

Friess, D.A., Rogers, K., Lovelock, C.E., et al., 2019. The state of the world's mangrove forests: past, present, and future. Annu. Rev. Env. Resour. 44 (1), 89–115. https://doi.org/10.1146/annurev-environ-101718-033302.

Gahir, S., Bharath, P., Raghavendra, A.S., 2021. Stomatal closure sets in motion long-term strategies of plant defense against microbial pathogens. Front. Plant Sci. 12. https://doi.org/10.3389/fpls.2021.761952.

Gatti, R.C., Di Paola, A., Bombelli, A., et al., 2017. Exploring the relationship between canopy height and terrestrial plant diversity. Plant Ecol. 218 (7), 899–908. https://doi.org/10.1007/s11258-017-0738-6.

Gholizadeh, A., Mišurec, J., Kopačková, V., et al., 2016. Assessment of red-edge position extraction techniques: a case study for Norway spruce Forests using HyMap and simulated Sentinel-2 data. Forests 7 (10), 226. https://doi.org/10.3390/f7100226.

Giri, C., Ochieng, E., Tieszen, L.L., et al., 2011. Status and distribution of mangrove forests of the world using earth observation satellite data. Glob. Ecol. Biogeogr. 20 (1), 154–159. https://doi.org/10.1111/j.1466-8238.2010.00584.x.

Gnanamoorthy P., Selvam V., Deb Burman P. K., et al. Seasonal variations of net ecosystem (CO_2) exchange in the Indian tropical mangrove forest of Pichavaram. Estuarine, Coastal and Shelf Science, 2020, 243: 106828. Doi: 10.1016/j.ecss.2020.106828.

Gomez, F.A., Lee, S.-K., Hernandez, F.J., et al., 2019. ENSO-induced co-variability of salinity, plankton biomass and coastal currents in the northern Gulf of Mexico. Sci. Rep. 9 (1), 178. https://doi.org/10.1038/s41598-018-36655-y.

Gou, R., Chi, J., Liu, J., et al., 2024. Atmospheric water demand constrains net ecosystem production in subtropical mangrove forests. J. Hydrol. 630, 130651. https://doi.org/10.1016/j.jhydrol.2024.130651.

Granados-Martínez, K.P., Yépez, E.A., Sánchez-Mejía, Z.M., et al., 2021. Environmental controls on the temporal evolution of energy and CO_2 fluxes on an arid mangrove of northwestern Mexico. J. Geophys. Res. Biogeo. 126 (7), e2020JG005932. https://doi.org/10.1029/2020JG005932.

Grossiord, C., Buckley, T.N., Cernusak, L.A., et al., 2020. Plant responses to rising vapor pressure deficit. New Phytol. 226 (6), 1550–1566. https://doi.org/10.1111/nph.16485.

Habib, E., Larson, B.F., Nuttle, W.K., et al., 2008. Effect of rainfall spatial variability and sampling on salinity prediction in an estuarine system. J. Hydrol. 350 (1), 56–67. https://doi.org/10.1016/j.jhydrol.2007.11.034.

Hang, L.M., Hung, B.X., Nga, N.T.T., et al., 2024. Evaluation of cloud masking methods using Sentinel-2 satellite images on Google Earth Engine: a case study in Vietnam. International Journal of Economic and Environmental Geology 15 (1), 26–32. https://doi.org/10.46660/ijeeg.v15i1.232.

Huffman G. J., Stocker E. F., Bolvin D. T., et al. GPM IMERG Final Precipitation L3 1 day 0.1 degree x 0.1 degree V07, Edited by Andrey Savtchenko, Greenbelt, MD, Goddard Earth Sciences Data and Information Services Center (GES DISC), 2023. Doi: 10.5067/GPM/IMERGDF/DAY/07.

Jia, M., Wang, Z., Mao, D., et al., 2023. Mapping global distribution of mangrove forests at 10-m resolution. Science Bulletin 68 (12), 1306–1316. https://doi.org/10.1016/j.scib.2023.05.004.

Jiang, G.-F., Goodale, U.M., Liu, Y.-Y., et al., 2017. Salt management strategy defines the stem and leaf hydraulic characteristics of six mangrove tree species. Tree Physiol. 37 (3), 389–401. https://doi.org/10.1093/treephys/tpw131.

Keith, H., Van Gorsel, E., Jacobsen, K.L., et al., 2012. Dynamics of carbon exchange in a Eucalyptus forest in response to interacting disturbance factors. Agric. For. Meteorol. 153, 67–81. https://doi.org/10.1016/j.agrformet.2011.07.019.

Kimera, F., Sobhi, B., Omara, M., et al., 2024. Impact of salinity gradients on seed germination, establishment, and growth of two dominant mangrove species along the Red Sea coastline. Plants 13 (24), 3471. https://doi.org/10.3390/plants13243471.

Kimirei, I.A., Igulu, M.M., Semba, M., et al., 2016. Small estuarine and non-estuarine mangrove ecosystems of Tanzania: overlooked coastal habitats? In: Diop, S., Scheren, P., Ferdinand Machiwa, J. (Eds.), Estuaries: A Lifeline of Ecosystem Services in the Western Indian Ocean. Estuaries of the World. Springer, Cham, pp. 209–226. https://doi.org/10.1007/978-3-319-25370-1_13.

Kirwan, M.L., Guntenspergen, G.R., Morris, J.T., 2009. Latitudinal trends in *Spartina alterniflora* productivity and the response of coastal marshes to global change. Glob. Chang. Biol. 15 (8), 1982–1989. https://doi.org/10.1111/j.1365-2486.2008.01834.x.

Knox, S.H., Bansal, S., Mcnicol, G., et al., 2021. Identifying dominant environmental predictors of freshwater wetland methane fluxes across diurnal to seasonal time scales. Glob. Chang. Biol. 27 (15), 3582–3604. https://doi.org/10.1111/gcb.15661.

Krauss, K.W., Ball, M.C., 2013. On the halophytic nature of mangroves. Trees 27 (1), 7–11. https://doi.org/10.1007/s00468-012-0767-7.

Krauss, K.W., Lovelock, C.E., Chen, L., et al., 2022. Mangroves provide blue carbon ecological value at a low freshwater cost. Sci. Rep. 12 (1), 17636. https://doi.org/10.1038/s41598-022-21514-8.

Krauss, K.W., Lovelock, C.E., Mckee, K.L., et al., 2008. Environmental drivers in mangrove establishment and early development: a review. Aquat. Bot. 89 (2), 105–127. https://doi.org/10.1016/j.aquabot.2007.12.014.

Lane, R.R., Day, J.W., Marx, B.D., et al., 2007. The effects of riverine discharge on temperature, salinity, suspended sediment and chlorophyll a in a Mississippi delta estuary measured using a flow-through system. Estuar. Coast. Shelf Sci. 74 (1), 145–154. https://doi.org/10.1016/j.ecss.2007.04.008.

Lellouche, J., Greiner, E., Bourdallé-Badie, R., et al., 2021. The Copernicus Global 1/12° Oceanic and Sea Ice GLORYS12 Reanalysis. Front. Earth Sci. 9, 2296–6463. https://doi.org/10.3389/feart.2021.698876.

Leopold, A., Marchand, C., Renchon, A., et al., 2016. Net ecosystem CO_2 exchange in the "Coeur de Voh" mangrove, New Caledonia: Effects of water stress on mangrove productivity in a semi-arid climate. Agric. For. Meteorol. 223, 217–232. https://doi.org/10.1016/j.agrformet.2016.04.006.

Li N., Zhang X., Xie Z., et al. Comparing different methods of calculating red-edge and blue-edge inflection position from hyperspectral data to early detect tree disease. proceedings of the IGARSS 2024 - 2024 IEEE International Geoscience and Remote Sensing Symposium, 2024, 10409-10412. Doi: 10.1109/IGARSS53475.2024.10642034.

Li, S.-L., Tan, T.-T., Fan, Y.-F., et al., 2022. Responses of leaf stomatal and mesophyll conductance to abiotic stress factors. J. Integr. Agric. 21 (10), 2787–2804. https://doi.org/10.1016/j.jia.2022.07.036.

Li, X., An, F., Wang, Y., et al., 2025. Comparative analysis of drought-driven water-use strategies in mangroves and forests. Forests 16 (3), 396. https://doi.org/10.3390/f16030396.

Liu, J., Lai, D.Y.F., 2019. Subtropical mangrove wetland is a stronger carbon dioxide sink in the dry than wet seasons. Agric. For. Meteorol. 278, 107644. https://doi.org/10.1016/j.agrformet.2019.107644.

Liu, Q., Wan, L., Xu, F., et al., 2025. Historical spatiotemporal trends in global mangrove productivity and its response to the environment: Perspectives from multiple satellite-based productivity proxies. Agric. For. Meteorol. 375, 110871. https://doi.org/10.1016/j.agrformet.2025.110871.

Liu, Y., Zhu, X., 2024. Tracking mangrove light use efficiency using normalized difference red edge index. Ecol. Ind. 168, 112774. https://doi.org/10.1016/j.ecolind.2024.112774.

López, J., Way, D.A., Sadok, W., 2021. Systemic effects of rising atmospheric vapor pressure deficit on plant physiology and productivity. Glob. Chang. Biol. 27 (9), 1704–1720. https://doi.org/10.1111/gcb.15548.

Lovelock, C.E., Bennion, V., De Oliveira, M., et al., 2024. Mangrove ecology guiding the use of mangroves as nature-based solutions. J. Ecol. 112 (11), 2510–2521. https://doi.org/10.1111/1365-2745.14383.

Lovelock, C.E., Cahoon, D.R., Friess, D.A., et al., 2015. The vulnerability of Indo-Pacific mangrove forests to sea-level rise. Nature 526 (7574), 559–563. https://doi.org/10.1038/nature15538.

Lovelock C. E., Krauss K. W., Osland M. J., et al. The physiology of mangrove trees with changing climate. The physiology of mangrove trees with changing climate. In: Goldstein, G., Santiago, L. (eds) Tropical Tree Physiology. Tree Physiology, vol 6. Springer, Cham, 2016. Doi: 10.1007/978-3-319-25370-1_13.

Luo, X., Croft, H., Chen, J.M., et al., 2019. Improved estimates of global terrestrial photosynthesis using information on leaf chlorophyll content. Glob. Chang. Biol. 25 (7), 2499–2514. https://doi.org/10.1111/gcb.14624.

Mckee, K.L., 2011. Biophysical controls on accretion and elevation change in Caribbean mangrove ecosystems. Estuar. Coast. Shelf Sci. 91 (4), 475–483. https://doi.org/10.1016/j.ecss.2010.05.001.

Mwangi, T., Kinyamario, J., Speybroeck, D., 2001. Photosynthesis and related physiological processes in two mangrove species, *Rhizophora mucronata* and *Ceriops tagal*, at Gazi Bay. Kenya. African Journal of Ecology 37, 180–193. https://doi.org/10.1046/j.1365-2028.1999.00167.x.

Nguyen, H.T., Stanton, D.E., Schmitz, N., et al., 2015. Growth responses of the mangrove *Avicennia marina* to salinity: development and function of shoot hydraulic systems require saline conditions. Ann. Bot. 115 (3), 397–407. https://doi.org/10.1093/aob/mcu257.

Parida, A., Jha, B., 2010. Salt tolerance mechanisms in mangroves: a review. Trees 24, 199–217. https://doi.org/10.1007/s00468-010-0417-x.

Pasquarella V. J., Brown C. F., Czerwinski W., et al. Comprehensive quality assessment of optical satellite imagery using weakly supervised video learning. proceedings of the 2023 IEEE/CVF Conference on Computer Vision and Pattern Recognition Workshops (CVPRW), 2023, 2125-2135. Doi: 10.1109/CVPRW59228.2023.00206.

Perri, S., Detto, M., Porporato, A., et al., 2023. Salinity-induced limits to mangrove canopy height. Glob. Ecol. Biogeogr. 32 (9), 1561–1574. https://doi.org/10.1111/geb.13720.

Perri, S., Katul, G.G., Molini, A., 2019. Xylem-phloem hydraulic coupling explains multiple osmoregulatory responses to salt stress. New Phytol. 224 (2), 644–662. https://doi.org/10.1111/nph.16072.

Reef, R., Lovelock, C.E., 2015. Regulation of water balance in mangroves. Ann. Bot. 115 (3), 385–395. https://doi.org/10.1093/aob/mcu174.

Rodda, S.R., Thumaty, K.C., Fararoda, R., et al., 2022. Unique characteristics of ecosystem CO_2 exchange in Sundarban mangrove forest and their relationship with environmental factors. Estuar. Coast. Shelf Sci. 267, 107764. https://doi.org/10.1016/j.ecss.2022.107764.

Roose, J.L., Frankel, L.K., Mummadisetti, M.P., et al., 2016. The extrinsic proteins of photosystem II: update. Planta 243, 889–908. https://doi.org/10.1007/s00425-015-2462-6.

Rosentreter, J.A., Laruelle, G.G., Bange, H.W., et al., 2023. Coastal vegetation and estuaries are collectively a greenhouse gas sink. Nat. Clim. Chang. 13 (6), 579–587. https://doi.org/10.1038/s41558-023-01682-9.

Rovai, A.S., Twilley, R.R., Castañeda-Moya, E., et al., 2018. Global controls on carbon storage in mangrove soils. Nat. Clim. Chang. 8 (6), 534–538. https://doi.org/10.1038/s41558-018-0162-5.

Rovai, A.S., Twilley, R.R., Castañeda-Moya, E., et al., 2021. Macroecological patterns of forest structure and allometric scaling in mangrove forests. Glob. Ecol. Biogeogr. 30 (5), 1000–1013. https://doi.org/10.1111/geb.13268.

Saintilan, N., Wilson, N.C., Rogers, K., et al., 2014. Mangrove expansion and salt marsh decline at mangrove poleward limits. Glob. Chang. Biol. 20 (1), 147–157. https://doi.org/10.1111/gcb.12341.

Sharma, S., Mackenzie, R.A., Tieng, T., et al., 2020. The impacts of degradation, deforestation and restoration on mangrove ecosystem carbon stocks across Cambodia. Sci. Total Environ. 706, 135416. https://doi.org/10.1016/j.scitotenv.2019.135416.

Shekhar, A., Hörtnagl, L., Buchmann, N., et al., 2023. Long-term changes in forest response to extreme atmospheric dryness. Glob. Chang. Biol. 29 (18), 5379–5396. https://doi.org/10.1111/gcb.16846.

Simard, M., Fatoyinbo, L., Smetanka, C., et al., 2019. Mangrove canopy height globally related to precipitation, temperature and cyclone frequency. Nat. Geosci. 12 (1), 40–45. https://doi.org/10.1038/s41561-018-0279-1.

Stocker T. Climate change 2013: the physical science basis: Working Group I contribution to the Fifth assessment report of the Intergovernmental Panel on Climate Change. Cambridge University Press, 2014. Doi: 10.1017/CBO9781107415324.

Su, J., Friess, D.A., Gasparatos, A., 2021. A meta-analysis of the ecological and economic outcomes of mangrove restoration. Nat. Commun. 12 (1), 5050. https://doi.org/10.1038/s41467-021-25349-1.

Sulman, B.N., Roman, D.T., Yi, K., et al., 2016. High atmospheric demand for water can limit forest carbon uptake and transpiration as severely as dry soil. Geophys. Res. Lett. 43 (18), 9686–9695. https://doi.org/10.1002/2016GL069416.

Ustin, S.L., Jacquemoud, S., 2020. How the optical properties of leaves modify the absorption and scattering of energy and enhance leaf functionality. In: Cavender-Bares, J., Gamon, J.A., Townsend, P.A. (Eds.), Remote Sensing of Plant Biodiversity. Springer, Cham, pp. 349–384. https://doi.org/10.1007/978-3-030-33157-3_14.

Vierra A., Razzaq A., Andreadis A. Chapter 27-Continuous variable analyses: t-test, Mann-Whitney U, Wilcoxon sign rank. Translational Surgery, 2023, 165-170. Doi: 10.1016/B978-0-323-90300-4.00045-8.

Wahid, S., Mainuddin, M., Chiew, F., et al., 2025. Salinity dynamics in the Sundarbans of Bangladesh: influence of climate, freshwater inflow, and sea level changes. Environ. Monit. Assess. 197 (11), 1219. https://doi.org/10.1007/s10661-025-14667-2.

Wang, X., Deng, Y., Liu, Y., et al., 2025. Increasing atmospheric dryness exacerbates mangrove carbon-water decoupling. New Phytol. 249 (1), 169–180. https://doi.org/10.1111/nph.70693.

Ward, R.D., Friess, D.A., Day, R.H., et al., 2016. Impacts of climate change on mangrove ecosystems: a region by region overview. Ecosyst. Health Sustainability 2 (4), e01211. https://doi.org/10.1002/ehs2.1211.

Xu, Z., Xiao, J., Chen, J., et al., 2025. Net carbon uptake during the wet seasons dominates ecosystem production in the northernmost mangroves in Southern China. J. Geophys. Res. Biogeo. 130 (11), e2025JG008769. https://doi.org/10.1029/2025JG008769.

Yang, S., Kang, R., Xu, T., et al., 2024. Improving satellite-based retrieval of maize leaf chlorophyll content by joint observation with UAV hyperspectral data. Drones 8 (12), 783. https://doi.org/10.3390/drones8120783.

Yi, P., Aoli, Z., Tinge, Z., et al., 2017. Using remotely sensed spectral reflectance to indicate leaf photosynthetic efficiency derived from active fluorescence measurements. J. Appl. Remote Sens. 11 (2), 026034. https://doi.org/10.1117/1.JRS.11.026034.

Yoo, J., Rohli, R.V., 2016. Global distribution of Köppen-Geiger climate types during the last Glacial Maximum, Mid-Holocene, and present. Palaeogeogr. Palaeoclimatol. Palaeoecol. 446, 326–337. https://doi.org/10.1016/j.palaeo.2015.12.010.

Yoshikai, M., Nakamura, T., Suwa, R., et al., 2022. Predicting mangrove forest dynamics across a soil salinity gradient using an individual-based vegetation model linked with plant hydraulics. Biogeosciences 19 (6), 1813–1832. https://doi.org/10.5194/bg-19-1813-2022.

Yuan, W., Zheng, Y., Piao, S., et al., 2019. Increased atmospheric vapor pressure deficit reduces global vegetation growth. Sci. Adv. 5 (8), eaax1396. https://doi.org/10.1126/sciadv.aax1396.

Zhang, W., Luo, G., Hamdi, R., et al., 2024a. Drought changes the dominant water stress on the grassland and forest production in the northern hemisphere. Agric. For. Meteorol. 345, 109831. https://doi.org/10.1016/j.agrformet.2023.109831.

Zhang, Z., Luo, X., Friess, D., et al., 2024b. Stronger increases but greater variability in global mangrove productivity compared to that of adjacent terrestrial forests. Nat. Ecol. Evol. 8 (2), 239–250. https://doi.org/10.1038/s41559-023-02264-w.

Zhao, X., Wang, C., Li, T., et al., 2022. Net CO_2 and CH_4 emissions from restored mangrove wetland: New insights based on a case study in estuary of the Pearl River. China. Science of the Total Environment 811, 151619. https://doi.org/10.1016/j.scitotenv.2021.151619.

Zheng, Y., Takeuchi, W., 2022. Estimating mangrove forest gross primary production by quantifying environmental stressors in the coastal area. Sci. Rep. 12 (1), 2238. https://doi.org/10.1038/s41598-022-06231-6.

Zhou, J.-J., Zhang, Y.-H., Han, Z.-M., et al., 2021. Evaluating the performance of hyperspectral leaf reflectance to detect water stress and estimation of photosynthetic capacities. Remote Sens. (Basel) 13 (11), 2160. https://doi.org/10.3390/rs13112160.

Zhu, X., Sun, C., Qin, Z., 2021. Drought-induced salinity enhancement weakens mangrove greenhouse gas cycling. J. Geophys. Res. Biogeo. 126 (8), e2021JG006416. https://doi.org/10.1029/2021JG006416.

Zhu, Z., Zhu, X., 2025. Increasing midday depression of mangrove photosynthesis with heat and drought stresses. Agric. For. Meteorol. 362, 110372. https://doi.org/10.1016/j.agrformet.2024.110372.